Insect Biochemistry and Molecular Biology 41 (2011) 178–190

Contents lists available at ScienceDirect

Insect Biochemistry and Molecular Biology

journal homepage: www.elsevier.com/locate/ibmb

Identification and characterization of functional aquaporin water channel protein from alimentary tract of whitefly, *Bemisia tabaci*

Lolita G. Mathew [a], Ewan M. Campbell [b], Andrea J. Yool [b], Jeffrey A. Fabrick [a,*]

[a] USDA-ARS, U.S. Arid Land Agricultural Research Center, 21881 North Cardon Lane, Maricopa, AZ 85138, USA
[b] University of Adelaide, School of Medical Sciences, Frome Rd., Medical School South, Adelaide, SA 5005, Australia

ARTICLE INFO

Article history:
Received 15 September 2010
Received in revised form
3 November 2010
Accepted 2 December 2010

Keywords:
Aquaporin
Bemisia tabaci
Filter chamber
Whitefly
Hemiptera
Phloem sap

ABSTRACT

Some hemipteran xylem and phloem-feeding insects have evolved specialized alimentary structures or filter chambers that rapidly transport water for excretion or osmoregulation. In the whitefly, *Bemisia tabaci*, mass movement of water through opposing alimentary tract tissues within the filter chamber is likely facilitated by an aquaporin protein. *B. tabaci* aquaporin-1 (BtAQP1) possesses characteristic aquaporin topology and conserved pore-forming residues found in water-specific aquaporins. As predicted for an integral transmembrane protein, recombinant BtAQP1 expressed in cultured insect cells localized within the plasma membrane. BtAQP1 is primarily expressed in early instar nymphs and adults, where in adults it is localized in the filter chamber and hindgut. *Xenopus* oocytes expressing BtAQP1 were water permeable and mercury-sensitive, both characteristics of classical water-specific aquaporins. These data support the hypothesis that BtAQP1 is a water transport protein within the specialized filter chamber of the alimentary tract and functions to translocate water across tissues for maintenance of osmotic pressure and/or excretion of excess dietary fluid.

Published by Elsevier Ltd.

1. Introduction

Hemipterans include both xylem and phloem feeders that ingest plant sap to meet their dietary requirements. Because plant xylem and phloem are nutritionally deficient, insects dependent on these solutions must typically ingest large quantities to achieve sufficient levels of nitrogen and other nutrients (Douglas, 2006). As a result of consuming large volumes of phloem or xylem, unique problems such as excess dietary fluid and regulating osmotic pressure must be overcome. Some hemipterans have circular midguts, with anterior and posterior extremities joining within specialized organs called filter chambers (Gullan and Cranston, 2005; Lehane and Billingsley, 1996). These structures are thought to help alleviate these physiological challenges.

Filter chambers are found in xylem feeders from families Cicadidae [*Quesada*: (Fonseca et al., 2010)], Cercopidae [*Philaenus* and *Aphrophora*: (LeCaherec et al., 1997)], and Cicadellidae [*Cicadella*: (Hubert et al., 1989; LeCaherec et al., 1997); *Euscelidius* and *Scaphoideus*: (LeCaherec et al., 1997)], as well as in phloem feeders from Aleyrodidae [whiteflies: (Cicero et al., 1995; Ghanim et al., 2001; Rosell et al., 2003)] and Eurymelidae [*Eurymela*: (Lindsay and Marshall, 1981; Marshall and Cheung, 1974)]. Only limited studies have been published to determine the directional flow of fluids and solutes through the alimentary tracts of phloem and xylem feeders. In *Cicadella* and *Eurymela*, injection of dye in various parts of the gut and hemolymph suggest that water moves directly from the anterior midgut, into the filter chamber, and into the hindgut (Cheung and Marshall, 1973; Lindsay and Marshall, 1981). Psyllids are phloem feeders and thought to excrete excess sap components through a filter chamber directly into the hindgut (Cicero et al., 2009). Although not definitively proven, it has been proposed that the whitefly filter chamber functions to shunt excess water and some solutes from the anterior digestive system directly to the hindgut (Cicero et al., 1995; Ghanim et al., 2001; Harris et al., 1996; Rosell et al., 2003; Salvucci et al., 1998). The rapid movement through adjacent tissues within the filter chamber suggests that highly water permeable cell membranes are present. Many biological membranes with high permeability facilitate water movement through water channel proteins or aquaporins [reviewed in (Benga, 2009; Campbell et al., 2008; Ishibashi et al., 2009; Maurel et al., 2008)].

Abbreviations: AQP, aquaporin; MIP, major intrinsic protein; BtAQP1, *Bemisia tabaci* aquaporin-1; TRITC, tetramethyl rhodamine isothiocyanate; PMSF, phenylmethylsulfonyl fluoride; eGFP, enhanced green fluorescent protein; cRNA, complementary RNA; TEA, tetraethylammonium; NPA motif, asparagine-proline-alanine motif; DRIP, *Drosophila* intrinsic protein; BIB, Big Brain protein; PRIP, *Pyrocoelia rufa* integral protein; TM, transmembrane.

* Corresponding author. Tel.: +1 520 316 6335; fax: +1 520 316 6330.
E-mail address: jeff.fabrick@ars.usda.edu (J.A. Fabrick).

0965-1748/$ – see front matter Published by Elsevier Ltd.
doi:10.1016/j.ibmb.2010.12.002

Aquaporins (AQPs) are members of the major intrinsic protein (MIP) family of integral membrane channel proteins found in most living organisms and facilitate mass transfer of water (and sometimes other substrates) across cell membranes for numerous essential physiological processes (Benga, 2009; Campbell et al., 2008; Gomes et al., 2009; Heymann and Engel, 1999; Yool, 2007). In invertebrates, these proteins have been involved in regulating movement of high volume liquid diets, cryoprotection and anhydrobiosis [a review on invertebrate aquaporins (Campbell et al., 2008)]. More recent publications report arthropod aquaporins in *Rhodnius prolixus* (Echevarria et al., 2001), *Acrythosiphon pisum* (Shakesby et al., 2009), *Rhipicephalus sanguineus* (Ball et al., 2009), and *Ixodes ricinus* (Campbell et al., 2010), all requiring high volume liquid diets. In the xylem feeder *Cicadella viridis*, AQPcic is localized in the filter chamber and functions as a water-specific channel to rapidly remove excess dietary fluid (LeCaherec et al., 1997). The phloem-feeding aphid, *A. pisum*, uses ApAQP1 to transfer dietary water across alimentary tract epithelium and is proposed to aid in osmoregulation of the midgut (Shakesby et al., 2009). AQPs are therefore important facilitators of water in the alimentary tracts of sap-feeding insects, where osmoregulation, concentration of dietary nutrients, and excretion of excess fluids are essential.

In addition to managing large quantities of water, sap-feeding insects also face other unique dietary challenges. For example, phloem feeders ingest sap with high concentration of sucrose, which can exceed 1 M (Douglas, 2006). The challenge for these insects is to prevent the osmolarity of the phloem sap from exceeding that of the hemolymph, which if not regulated can result in mass transfer of water into the gut, resulting in osmotic collapse and desiccation. Phloem-feeding insects have not only evolved specialized alimentary morphology, but also biochemical processing of carbohydrates to mediate adverse conditions. In both aphids and whiteflies, biochemical conversions of sucrose to oligosaccharides and/or other carbohydrates with reduced osmotic potential may alter osmoregulatory properties of the dietary ingesta (Byrne et al., 2003; Douglas, 2006; Hendrix and Salvucci, 1998, 2001; Salvucci, 2003; Salvucci and Crafts-Brandner, 2000; Salvucci et al., 1999, 1997; Wolfe et al., 1998).

In this paper, we describe the characterization of an aquaporin, BtAQP1, from *Bemisia tabaci* (Gennadius) (Hemiptera: Aleyrodidae), a major polyphagous phloem-feeding insect pest of food, fiber, and ornamental crops. Based on sequence conservation, bioinformatic predictions, cellular and tissue localization, temporal expression, and functional analysis, BtAQP1 is a water-specific aquaporin that plays an important role in water regulation within the alimentary system. Finally, we contrast those differences proposed for movement of dietary water in several xylem and phloem feeders with known functional aquaporins.

2. Materials and methods

2.1. Insects

A colony of *B. tabaci* Biotype B (Gennadius) were mass-reared on *Brassica oleracea* in 35″ × 35″ × 85″ cages within a glasshouse maintained at 29 °C.

2.2. cDNA isolation and 5′-RACE of BtAQP1

Total RNA was extracted from 100 mg of *B. tabaci* adults using TRIzol® reagent (Invitrogen, Carlsbad, CA USA). cDNA was produced using random hexamer primers and SuperScript III First-strand Synthesis System (Invitrogen, Carlsbad, CA USA) according to manufacturer's recommendations. Several sets of degenerate PCR primers were designed from conserved regions identified in Vector NTI AlignX multiple sequence alignment of AQPs from *Aedes aegypti* (AF219314.1), *Drosophila melanogaster* (NM_165833.2), *Haematobia irritans* (U51638.1), *Apis mellifera* (XM_624528.1), *Bombyx mori* (NM_001043454.1), *C. viridis* (X97159.1), and *Tribolium castaneum* (XM_963249.2). A ~400 bp fragment was amplified using primers 2BtAQP5 (5′-CACATCAAYCCMGCBGTCAC-3′) and 8BtAQP3 (5′-GGN CCCRCCCARTAMACCCA-3′), each corresponding to asparagine-proline-alanine (NPA) motifs highly conserved in many AQPs and ligated into pCR2.1-TOPO using TOPO TA Cloning Kit (Invitrogen, Carlsbad, CA USA). Plasmid DNA was propagated in OneShot TOP10 Electrocompetent *Escherichia coli* and purified using QIAprep Spin MiniPrep Kit (Qiagen, Valencia, CA USA). Inserts were sequenced with T7 and M13 Reverse vector primers using the GenomeLab™ DTCS Quick Start Kit on a CEQ8000 DNA Sequencer (Beckman-Coulter, Brea, CA USA).

The 5′ and 3′ ends of BtAQP1 were identified through rapid amplification of cDNA ends (RACE) using the GeneRacer™ kit (Invitrogen, Carlsbad, CA USA). For 5′-RACE, two antisense primers (13BtAQP5: 5′-AACATGTCCCGACACAGCTAGTCCA-3′ and 14BtAQP3: 5′-ACCAGCAGCCGTGTAACCTGTTTTT-3′) were designed from the 438 bp partial BtAQP1 clone and used with GeneRacer 5′-primer. Fully-nested PCR was used for 3′-RACE, with the first reaction using 10BtAQP5 (5′-TAACTTGTGGACTAGCTGTGTCGGGACA-3′) and GeneRacer 3′-primer and the second round of PCR using 9BtAQP5 (5′-CCTTGGAGCCATCTGTGGAGCAATCA-3′) and GeneRacer 3′-nested primer. PCR products were sub-cloned into pCR2.1-TOPO and sequenced as indicated above.

The full-length BtAQP1 open reading frame (ORF) was confirmed by PCR amplification from *B. tabaci* cDNA using 16AQUA5 (5′-ATGGA GGACATATCATCTTCCGGCGAAG-3′) and 15AQUA3 (5′-GAAATCATA AGAGCTCTCATCCGATCT-3′) and sub-cloned into pCR2.1-TOPO.

2.3. Bioinformatics and phylogeny

Sequences were analyzed in Vector NTI (Invitrogen, Carlsbad, CA USA) and comparison of BtAQP1 sequence against the non-redundant public sequence database was made using BLAST search programs (Altschul et al., 1990). Sequence analysis tools of the ExPASy Molecular Biology Server of Swiss Institute of Bioinformatics, including Translate, Compute pI/MW, and TMHMM, were used to analyze the deduced BtAQP1 protein sequence. Multiple sequence alignments were performed using CLUSTALW (Larkin et al., 2007), AlignX from Vector NTI or Network Protein Sequence Analysis (NPS) (Combet et al., 2000). Phylogenetic analysis using predicted AQP protein sequences was performed with the unweighted pair group method with arithmetic mean (UPGMA, Sneath and Sokal, 1973), neighbor-joining (Saitou and Nei, 1987), minimum evolution and maximum parsimony (Saitou and Nei, 1986) methods and trees were constructed with 10,000 bootstrap replicates using MEGA 4 (Tamura et al., 2007). Only the UPGMA tree is represented as all trees were similar in phylogeny. Glycosylation predictions were made using post-translational modification servers found at the Center for Biological Sequence Analysis (http://www.cbs.dtu.dk/services/).

2.4. Computational molecular modeling

To build model structures for BtAQP1, automated protein homology-based molecular modeling software was used [SWISS-MODEL, (Arnold et al., 2006; Kiefer et al., 2009; Peitsch, 1995); I-TASSER (Roy et al., 2010; Zhang, 2008, 2009) and Geno 3D, (Combet et al., 2002)]. Rat aquaporin 4 (PDB ID: 2D57) and human AQP5 (PDB ID: 3D9S) were the top threading templates used for automated modeling analyses using SWISS-MODEL and I-TASSER, respectively. BtAQP1 was also modeled in I-TASSER using 2D57 as template. Structures used as templates in Geno 3D included 2D57, *Bos taurus*

AQP1 (PDB ID: 1J4N) and AQP0 (PDB ID: 2B6P), and human AQP1 (PDB ID: 1FQY and PDB ID: 1H6I). The overall stereochemical quality of the Geno 3D models were assessed by Ramchandran plot analysis using PROCHECK (Combet et al., 2002; Laskowski et al., 1993). RasMol V2.7.4.2 Molecular Graphics Visualization Tool was used to visualize the three-dimensional coordinates for the atoms of the model (http://rasmol.org/).

2.5. RNA extraction and semi-quantitative reverse transcription PCR

A few hundred *B. tabaci* adults were introduced into clip cages and allowed to lay eggs on broccoli leaves over a 48 h period to synchronize hatching. Whiteflies representing each stage (egg, 1st instar, 2nd–3rd instar, 4th instar-pupa and adult) were collected and frozen at −80 °C. Tissue samples were homogenized using Kontes pestles (Fisher Scientific, Pittsburg, PA USA) and total RNA was extracted using TRIzol® reagent (Invitrogen, Carlsbad, CA USA). Total RNA was treated with DNA-free™ DNase (Ambion, Austin, TX USA) to remove genomic DNA contamination, if any, carried over during total RNA extraction. Integrity of the total RNA was confirmed on the Agilent 2100 Bioanalyzer using the RNA Nano 6000 LabChip kit (Agilent Technologies, Santa Clara, CA USA) according to manufacturer's instructions.

RNA concentration was determined using NanoDrop ND1000 spectrophotometer (NanoDrop Technologies/Thermo Scientific, Wilmington, DE USA). Samples were diluted and 1.5 μg of total RNA was used to prepare cDNA using random decamer primers according to the protocol described in RETROscript Kit (Ambion, Austin, TX USA). For RT-PCR reactions, BtAQP1-specific primers 16AQUA5 and 15AQUA3 were used to amplify the 786 bp full-length ORF. The appropriate number of PCR cycles was determined empirically and included 20, 22, 25 and 30 cycles. PCR products were analyzed using the Agilent 2100 Bioanalyzer with DNA 7500 LabChip kit (Agilent Technologies, Santa Clara, CA USA) according to the manufacturer's protocol.

2.6. Antibody production

A synthetic peptide (IMP-1) corresponding to the final 16 residues of BtAQP1 (C-ITFKAKKRSDESSYDF) was identified by Pacific Immunology (Ramona, CA USA) to be potentially immunogenic. IMP-1 was synthesized, conjugated to Keyhole Limpet Hemocyanin (KLH) carrier protein, and used to immunize two rabbits (Pacific Immunology, Ramona, CA USA). Monospecific antibody was purified from pooled serum from the two immunized rabbits (2965/2966), hereafter referred to as anti-BtAQP1, using covalently-coupled IMP-1 peptide affinity column.

2.7. Immunoblot and immunofluorescence analysis of B. tabaci tissues

B. tabaci adults ($n = 40$) were collected and either used as whole body or dissected to separate gut, head, leg and whole body without gut in dissection buffer [10 mM Tris–HCl, pH 7.4, 0.15 M NaCl, 0.01% Triton X-100, 0.4 mM phenylmethylsulfonyl fluoride (PMSF)] under stereomicroscope. Tissues were homogenized using Kontes pestles (Fisher Scientific, Pittsburg, PA USA) and equal volumes of homogenates were separated by 10% sodium dodecyl sulfate-polyacrylamide gel electrophoresis (SDS-PAGE) using NuPAGE Pre-Cast Gel System (Invitrogen, Carlsbad, CA USA). Proteins were transferred to nitrocellulose and probed with 1:500 diluted affinity-purified rabbit anti-BtAQP1 antibody. The secondary antibody consisted of 1:3000 diluted goat anti-rabbit IgG with alkaline phosphatase (AP) conjugate (Bio-Rad, Hercules, CA USA) and bands were developed using Bio-Rad AP Conjugate Substrate Kit.

For immunofluorescence, *B. tabaci* gut tracts were dissected from adults ($n = 20$) in dissection buffer under stereomicroscope. Tissues were washed twice with phosphate buffered saline (PBS) and fixed in 10% neutral buffered formalin at 4 °C overnight. Tissues were washed gently twice with PBS and permeabilized and blocked with 0.1% Triton X-100 in PBS containing 10% Fetal Bovine Serum (FBS) for 2 h at 23 °C. Gut tissues were incubated with affinity-purified rabbit anti-BtAQP1 primary antibody (1:50 dilution) for 1 h at 23 °C and then washed three times with PBS. Final incubation was followed for 1 h with secondary antibody, Rhodamine (TRITC)-conjugated goat anti-rabbit IgG (Southern Biotech, Birmingham, AL USA) (1:400 dilution). The tissues were washed three times with PBS and analyzed using Olympus FSX 100 with G excitation (Ex530-550 Em475IF) equivalent to U-MWIG3 filter set for TRITC to localize the BtAQP1 antibody. Negative control gut tracts were similarly handled, but lacked incubation with anti-BtAQP1 antibody.

2.8. Expression of BtAQP1 in Sf9 cell culture and immunofluorescence microscopy

Overlap extension PCR was used to construct the chimeric expression plasmid, eGFP-BtAQP1/pIB, by fusing the enhanced green fluorescent protein (eGFP) coding sequence (CDS) to the region encoding the amino terminus of BtAQP1. The first PCR amplified the eGFP CDS from p3X3P3-eGFP using the gene-specific primer, LM1eGFP5 (5′-GTTATGGTGAGCAAGGGCGA-3′) and the chimeric antisense primer, LM6BtAQP1-eGFP3 (5′-GAAGATGA-TATGTCCTCCATcttgtacagctcgtccatgc-3′). The second PCR amplified the complete coding region of the BtAQP1 and the stop codon from the plasmid, BtAQP1/pCR2.1-TOPO, by using the chimeric sense primer, LM5eGFP-BtAQP5 (5′-gcatggacgagctgtacaagATGGAGGACA-TATCATCTTC-3′) and the BtAQP1 antisense primer LM3BtAQP3. The final step involved PCR amplification using the two previous reactions as templates with the eGFP gene-specific sense primer LM1eGFP5 and the BtAQP1-specific antisense primer LM3BtAQP3. The resulting PCR product was sub-cloned into the expression vector pIB/V5-His-TOPO (Invitrogen, Carlsbad, CA USA) and sequenced to confirm the presence and orientation of insert. Takara Ex Taq (Takara Bio USA, Madison, WI USA) was used for all PCR amplifications.

The construct eGFP-BtAQP1-TR#1/pIB lacking the final 16 carboxyl-terminal residues (ITFKAKKRSDESSYDF) was prepared by PCR amplification from eGFP-BtAQP1/pIB template using LM1 eGFP5 and LM4BtAQP3 (5′-ttaGGCGTAAAGCAGACTGGCAGT-3′), which introduces a premature stop codon at position 247. A control expression plasmid (pIB/eGFP) lacking BtAQP1 was used.

Transfections were performed according to the Insect GeneJuice transfection reagent protocol (Novagen/EMD Biosciences, Madison, WI USA) using adherent monolayer Sf9 cells and ~2.0 μg of plasmid per transfection. One day post transfection, fresh media containing 10 μg μl^{-1} gentamycin was added and cells were maintained for 24 h at 27 °C.

Immunofluorescence was performed using Olympus FSX 100 fluorescence microscope and anti-BtAQP1 antibody. Transfected Sf9 cells grown on 35 mm glass bottom petri dishes were washed twice with PBS and fixed in 10% neutral buffered formalin for 20 min. Cells were permeabilized and blocked with 0.1% Triton X-100 in PBS containing 10% FBS for 1 h at 23 °C. Cells were incubated with 1:50 diluted anti-BtAQP1 for 1 h at 23 °C. Sf9 cells were washed three times with PBS and incubated for 1 h with 1 μg of the secondary antibody, Rhodamine (TRITC)-conjugated goat anti-rabbit IgG (Southern Biotech, Birmingham, AL USA) per 1×10^6 cells. Cells were washed three times with PBS and analyzed for TRITC and eGFP with

B excitation (Ex460-495 Em510-550 DM505) and G excitation (Ex530-550 E475IF DM570) filters, respectively.

2.9. cRNA synthesis, Xenopus oocyte expression and permeability assays

BtAQP1 ORF was sub-cloned into a modified *Xenopus laevis* β-globin plasmid expression vector (Anthony et al., 2000), linearized with *SacII*, and transcribed *in vitro* (T3 mMessage mMachine; Ambion, Austin, TX USA). *In vitro*-transcribed complementary RNA (cRNA) corresponded to the full-length ORF (residues 1–262) for BtAQP1. cRNA (at 20 ng μL^{-1}) was resuspended in sterile water. cDNA for human AQP1 was provided by *P. Agre* (Preston et al., 1992; accession number NM_198098), linearized with *BamHI* and transcribed with T3 polymerase. cDNA for Plasmodium PfAQP was provided by E. Beitz (Hansen et al., 2002; accession number AJ413249), linearized with *NotI* and transcribed with T7 polymerase.

Unfertilized *X. laevis* oocytes were defolliculated with collagenase (type 1A, 1.5 mg mL^{-1}; Sigma, St. Louis, MO) and trypsin inhibitor (15 mg mL^{-1}) in OR-2 saline [82 mM NaCl, 2.5 mM KCl, 1 mM $MgCl_2$, and 5 mM 4-(2-Hydroxyethyl)piperazine-1-ethanesulfonic acid (HEPES)] at 18 °C for 1.5 h, washed in OR-2 saline solution, and maintained in ND96 saline (96 mM NaCl, 2 mM KCl, 1 mM $MgCl_2$, 1.8 mM $CaCl_2$, 5 mM HEPES, pH 7.55) supplemented with penicillin and streptomycin, and 10% (V/V) heat-inactivated horse serum. Oocytes were injected with 50 nL of water containing 1 ng of BtAQP1 cRNA and were incubated for 2 or more days at 18 °C to allow protein expression.

For quantitative swelling assays, oocytes were incubated in isotonic ND96 saline (without serum or antibiotics) for 1–2 h at room temperature and were tested for water permeability by swelling in 50% hypotonic saline (isotonic diluted with an equal volume of water). Glycerol permeability was assayed by measuring swelling rates of oocytes in saline in which 65 mM NaCl had been iso-osmotically replaced with glycerol. Inhibitory effects of mercury (Hg) or tetraethylammonium (TEA) chloride were tested by preincubation of injected oocytes in isotonic saline containing either 1 mM $HgCl_2$ or 100 μM TEA for 15 min prior to swelling assays. For TEA-preincubated oocytes, TEA also was included at 100 μM in the hypotonic swelling solutions. Swelling rates were quantified by relative increases in oocyte cross-sectional area imaged by video microscopy (charge-coupled device camera; Cohu, San Diego, CA) at 0.5 frames per s for 45 s using NIH ImageJ software. Rates were measured as described previously (Anthony et al., 2000; Boassa and Yool, 2003) using Prism (GraphPad Software Inc., San Diego, CA). Data for cross-sectional oocyte area (A) standardized to the initial area (Ao) as a function of time were fit by linear regression to determine the swelling rate from the slope value (%A/Ao $s^{-1} \times 10^3$). All surgical procedures were approved by the University of Adelaide Animal Ethics committee and the procedures followed protocols approved under the Australian Code of Practice for the Care and Use of Animals for Scientific Purposes.

3. Results

3.1. Cloning, topology and homology of BtAQP1

Degenerate primers based on conserved regions from several insect aquaporins were used to PCR amplify a 438 bp partial fragment from *B. tabaci* cDNA. The cloned fragment was sequenced and BLAST analysis revealed high similarity with the aquaporin superfamily (data not shown). Using the sequence from the partial clone, we identified the 5′ and 3′ end of putative AQP by RACE and full-length BtAQP1 ORF (789 bp) was amplified from cDNA and sub-cloned. The coding sequence of BtAQP1 (Accession no. EU127479.1) consists of 262 amino acids with a predicted molecular weight of 27 kDa (Fig. 1A) and with isoelectric point of 6.5. No putative N- or O-glycosylation sites were identified for BtAQP1.

Topology and hydrophobicity predictions using TMHMM program revealed that BtAQP1 consists of six transmembrane-spanning regions and intracellular amino and carboxyl termini (Fig. 1A and B), fitting the pattern known for other members of the aquaporin superfamily. Comparison of predicted topology and amino acid sequence of BtAQP1 with other insect and mammalian aquaporins reveal several key features that are common to members of the aquaporin superfamily, including six transmembrane domains, five alternating extracellular/intracellular loop regions, intracellular amino and carboxyl termini and two NPA motifs.

Three-dimensional structures are not yet available for arthropod aquaporins. Homology model predictions from SWISS-MODEL, I-TASSER, and Geno 3D using crystallography coordinates of *Rattus norvegicus* aquaporin 4 [PDB ID: 2D57; (Hiroaki et al., 2006)] as a structural template depicted high similarity with BtAQP1 (49.5% identity) and reliable predicted model structures (SWISS-MODEL Ramachandran plot = 81.7% residues in favorable region, 15.7% in allowable region, 2.6% in generously allowed region, and 0.0% in disallowed region; I-TASSER: c-score = −0.09, TM-score = 0.70 ± 0.12, RMSD = 6.1 ± 3.8; Geno 3D: Model energy = −8356 kcal mol^{-1}, Ramachandran plot = 79.1% residues in favorable region, 16.6% in allowable region, 4.8% in generously allowed region, and 0.0% in disallowed region). Fig. 1C shows predicted BtAQP1 model from Geno 3D using 2D57 as template. All models show two tandem structural repeats, each consisting of three transmembrane helices (TM1-3 and TM4-5) and a short α-helix in loops B and E each containing an NPA motif predicted to line one side of the pore. This conserved structure is called the "aquaporin fold" (Murata et al., 2000). Residues that comprise the Ar/R constriction (Phe-71, His-198, Ala-207, and Arg-213) are found in BtAQP1 and are predicted to project into the putative cytoplasmic pore opening (Fig. 1A and C) and establish water selectivity.

We used CLUSTALW and MEGA 4.0 phylogenetic analysis to compare BtAQP1 with other insect aquaporins (Fig. 2). Phylogenetic analysis of full-length AQP cDNA clones retrieved from GenBank reveals the existence three distinct families of insect AQPs, including *Drosophila* intrinsic proteins (DRIPs), Big Brain proteins (BIBs), and *Pyrocoelia rufa* integral proteins (PRIPs) as well as two unique sequences yet to be placed in a defined subfamily (Fig. 2; Campbell et al., 2008). Multiple insect AQP subfamilies other than DRIPs, PRIPs, and BIBs likely exist based on the phylogenetic analysis using cDNA and putative genomic AQP sequences (data not shown). BtAQP1 clustered with the known or predicted DRIP family of proteins (Campbell et al., 2008) and overall shares 31% similarity with shown members of that family. BtAQP1 was most closely related to AQPs from the hemipteran leafhopper, *C. viridis* (54% identity), the human body louse, *Pediculus humanus corporis* (52% identity), and a putative AQP from the termite *Coptotermes formosanus* (53% identity). Interestingly, two splice variant AQPs from the pea aphid, *A. pisum* (ApAQP1 and 2) cluster together on a separate branch, indicating divergence from other insect DRIPs (41 and 43% identity to BtAQP1, respectively) (Fig. 2 and Supplemental Fig. S1). Among the human AQPs, BtAQP1 is most similar to AQP4 (P55087.2), sharing 40% identity and key conserved sequence motifs that are critical for water permeability (Supplemental Fig. S2A and B).

3.2. Temporal expression and localization of BtAQP1

We investigated the expression pattern of BtAQP1 transcripts over the life cycle of *B. tabaci* including egg, 4 nymphal stages (1st instar or crawler, 2nd, 3rd, 4th instar), pupal stage and adult.

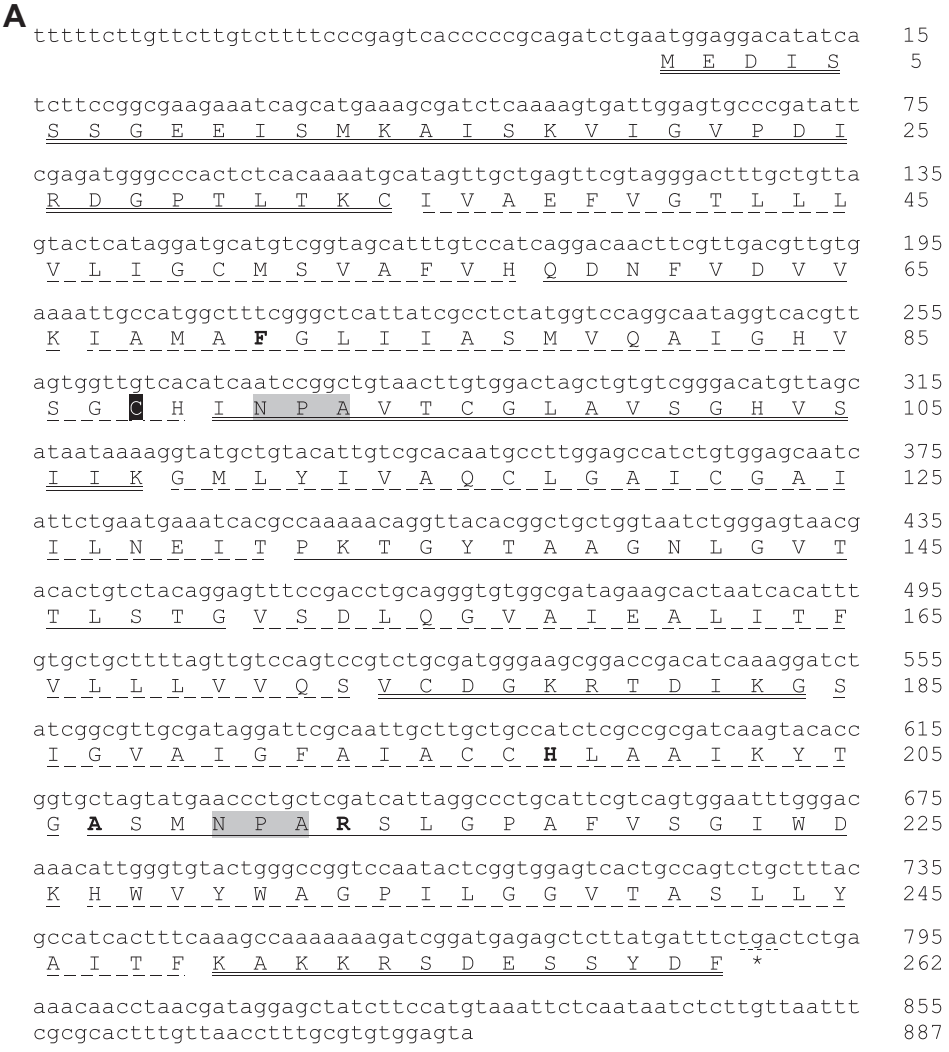

Fig. 1. Sequence analysis, predicted topology, and homology modeling of BtAQP1. (A) Nucleotide and deduced amino acid sequence of BtAQP1. Predicted topology is indicated under amino acid translation, with intracellular domains indicated by *double underline*, transmembrane helices with *dashed underline*, and extracellular domains indicated with *single underline*. The NPA boxes are shown with grey highlight and residues that comprise the Ar/R constriction (Phe-71, His-198, Ala-207, and Arg-213) are shown in bold. Predicted mercury-sensitive cysteine (Cys-88) is shown with white text on black highlight. (B) Prediction of intra/extracellular domains and transmembrane helices using TMHMM Server v. 2.0. Labels indicate transmembrane domains (TM1-6), loop regions (A–E), and amino (N-term) or carboxyl (C-term) terminal ends. (C) Geno 3D homology model of BtAQP1 using the crystal structure of rat aquaporin 4 (PDB ID: 2D57) as template. Structure on left viewed parallel to the plane of the membrane with inside the cell down. Intracellular (B and D) and extracellular (A, C, and E) loops and transmembrane helices are shown (TM1 in red; TM2 in orange; TM3 in yellow; TM4 in green; TM5 in blue; TM6 in purple). Structure on right viewed perpendicular to the axis of the pore from the extracellular side of the membrane. NPA motifs are shown in pink space fill and Ar/R residues (Phe-71, His-198, Ala-207, and Arg-213) are shown in green stick representation with van der Waals' surface shown in dots.

Using semi-quantitative PCR, BtAQP1 amplicons were analyzed at 20, 22, 25 and 30 cycles using Bioanalyzer. We observed that BtAQP1 transcripts were most highly expressed in 2nd instar nymphs and least present in eggs (Fig. 3, cycle 22). BtAQP1 transcript abundance was also low in 4th instar nymphs and pupae (Fig. 3, compare cycles 22 and 25) with intermediate levels in 1st instar crawlers, 3rd instar nymphs, and adults (Fig. 3, cycle 22).

Cellular localization of BtAQP1 was determined using heterologous expression in Sf9 cells producing chimeric GFP-labeled BtAQP1. The anti-BtAQP1 antibody bound specifically to recombinant BtAQP1 expressed in insect cells co-expressing GFP (compare Fig. 4B and C). Anti-BtAQP1 antibody did not bind to truncated recombinant BtAQP1 lacking final carboxyl-terminal 16 amino acid residues (ITFKAKKRS-DESSYDF) against which anti-BtAQP1 was made (Fig. 4F and G). Fluorescence microscopy revealed that recombinant BtAQP1 is produced and transported to the plasma membrane in Sf9 cells (Fig. 4I and J) even though BtAQP1 is partially localized within the intracellular vesicles. Interestingly, the truncated BtAQP1 was primarily intracellular and not found in the plasma membrane, as indicated by the lack of fluorescence in plasma membranes between adjacent cells (compare boxed areas between Fig. 4I and K which shows plasma membranes overlapped between two adjacent cells; note lack of expression in the overlapped plasma membrane in Fig. 4K and L). No red fluorescence was observed in transfected cells expressing GFP-BtAQP1 chimera when probed with secondary antibody alone, indicating specificity of anti-BtAQP1 (data not shown).

To localize BtAQP1 within adults, head, leg and gut tissue was isolated and tested by immunoblot analysis using anti-BtAQP1. Several immunoreactive bands were detected in gut homogenate with two major bands at approximately 19–22 kDa and two faint bands with predicted mass less than 10 kDa (Fig. 5, Lane 3). No bands were detected in homogenates from heads or legs. Homogenates from adults with gut tracts removed showed very faint bands (Fig. 5, Lane 4), indicating that BtAQP1 is primarily

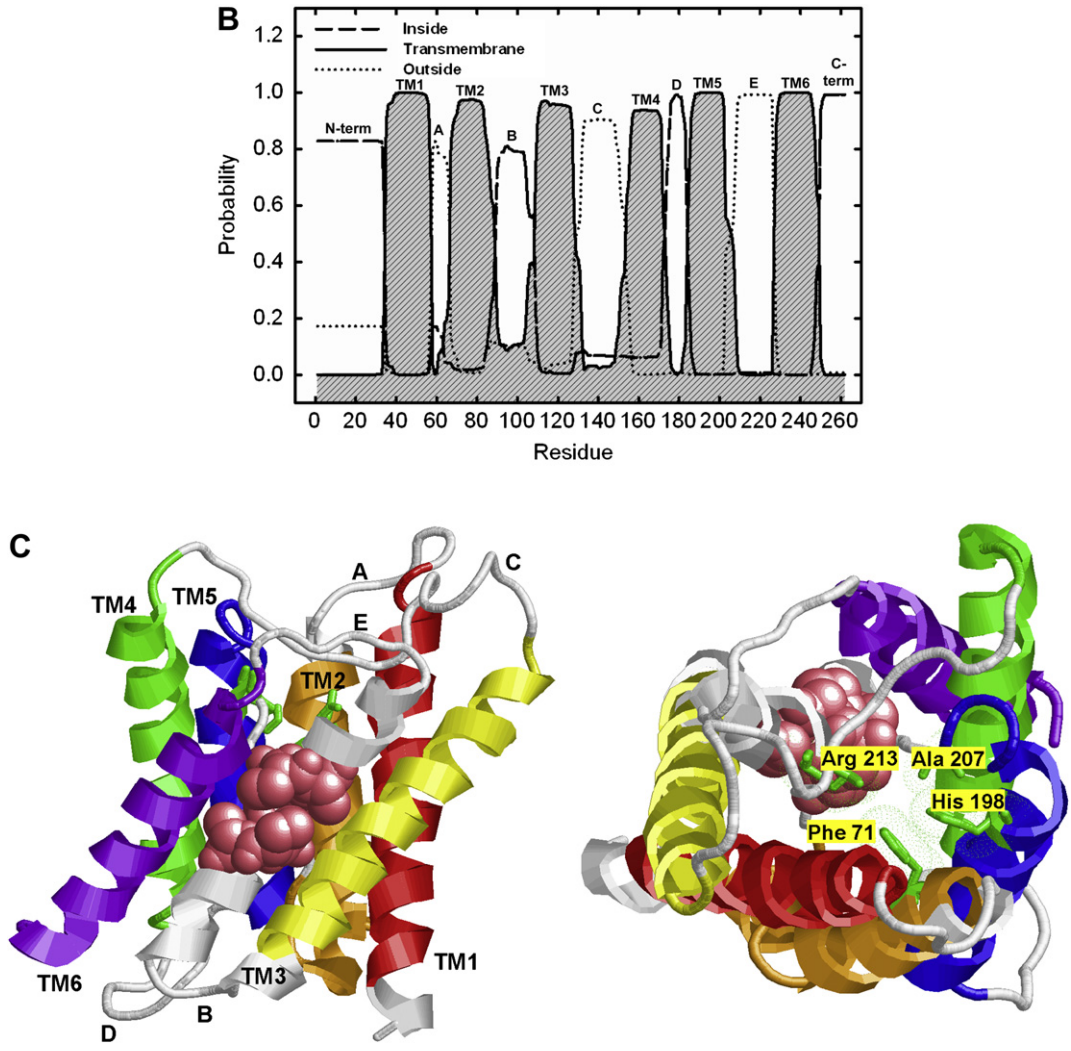

Fig. 1. (*continued*).

expressed within the gut. Gut homogenates separated by SDS-PAGE and stained with Coomassie show numerous faint bands ranging in size from 10 to 100 kDa, with several faint bands visible between 19 and 22 kDa (data not shown). Lack of immunoreactive bands in head tissue and bodies with gut tracts removed indicates little or no expression of BtAQP1 in other tissues (Fig. 5).

The expression and localization of BtAQP1 in gut tissues of *B. tabaci* was further investigated by immunohistochemistry (Fig. 6). Dissected guts treated with anti-BtAQP1 and Rhodamine (TRITC)-conjugated goat anti-rabbit IgG secondary antibody showed intense staining within the filter chamber (Fig. 6B and C) and in the anterior ileum portion of the hindgut (Fig. 6B, C, E and F). No fluorescence was observed in the external esophagus, caeca, connecting chamber, ascending or descending midguts (Fig. 6B, C, E and F). Although alimentary tract preparations frequently lacked intact posterior hindguts (including ileum, colon and rectal sac) and foreguts (including salivary glands), these tissues did not fluoresce when independently dissected (data not shown). A portion of the external esophagus lacking fluorescence is shown in Fig. 6E and F. Gut tissue probed directly with the secondary antibody without incubation in primary antibody (anti-BtAQP1) showed no fluorescence (data not shown).

3.3. Oocyte functional analysis

The functions of BtAQP1 in water and glycerol transport were tested using the *Xenopus* oocyte expression system, measuring volume changes indicative of net influx of water or glycerol in hypotonic and isotonic solutions, respectively (Fig. 7A). We observed 16-fold ($p < 0.001$) higher swelling rates (mean ± SEM 48 ± 3.2 % $A/A_0 \times 1000 \times s^{-1}$) in BtAQP1-injected oocytes compared to water-injected oocytes (3.0 ± 2.8 $\%A/A_0 \times 1000 \times s^{-1}$) (Fig. 7B). Likewise, oocytes expressing the human aquaporin1 (AQP1) water channel protein swelled at a rate (39 ± 1.7 $\%A/A_0 \times 1000 \times s^{-1}$) significantly ($p < 0.001$) higher than that of control oocytes not expressing aquaporin. We tested BtAQP1 for sensitivity to block by known AQP inhibitors such as mercuric chloride ($HgCl_2$) and tetraethylammonium (TEA) chloride (Fig. 7B). Preincubation of BtAQP1-injected oocytes in 1 mM $HgCl_2$ reduced water permeability by 76% ($p < 0.001$) compared to water control oocytes, confirming its sensitivity to mercury. One hundred micromolar TEA did not significantly ($p = 0.295$) reduce water permeability in BtAQP1-injected oocytes. Furthermore, BtAQP1-injected oocytes showed no appreciable transport of glycerol (6.8 ± 2.0 $\%A/A_0 \times 1000 \times s^{-1}$), in contrast to the known glycerol transporter, *Plasmodium falciparum* aquaglyceroporin (33 ± 2.4 $\%A/A_0 \times 1000 \times s^{-1}$) (Hansen et al., 2002) (Fig. 7C).

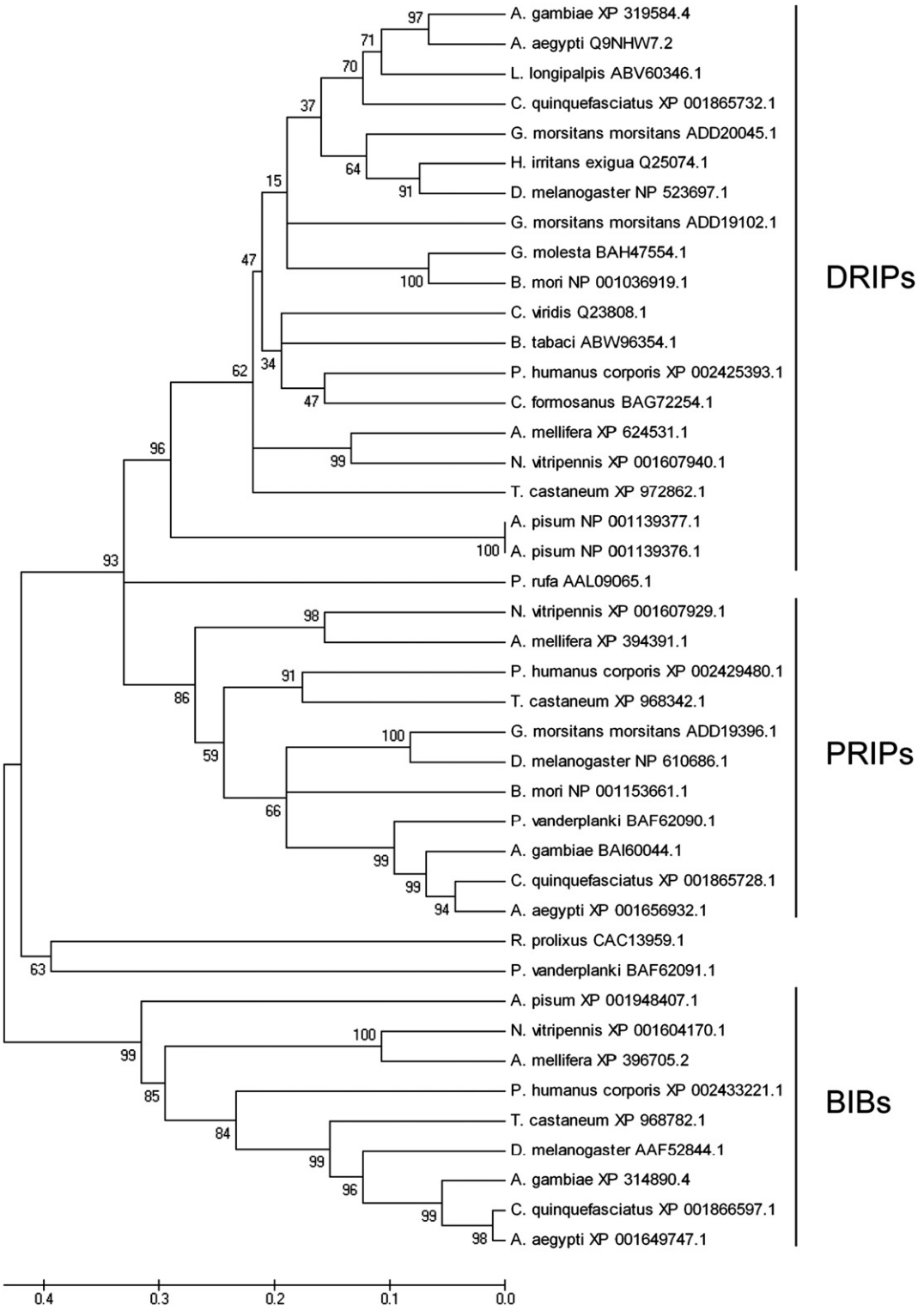

Fig. 2. Phylogenetic analysis of BtAQP1 and other insect aquaporins. BtAQP1 amino acid sequence was compared with other aquaporins using UPGMA method and phylogenetic tree was constructed using MEGA 4.0. Scale bar shows an estimate of the number of amino acid substitution per site. Numbers on the branches are the bootstrap values obtained from 10,000 replicates. Taxonomic name and accession number for each sequence is given. Representatives from three major families (DRIPs, PRIPs, and BIBs) are shown.

4. Discussion

Aquaporins are integral membrane proteins belonging to a large family of water channel proteins that assist in rapid movement of water across cellular membranes (Benga, 2009). Because water and solute transport are universal requirements for living cells, these proteins are found in most living organisms. The water channel protein family is part of the major intrinsic protein (MIP) superfamily of proteins (Benga, 2009). A number of aquaporin water channel proteins have been identified in invertebrates, including at

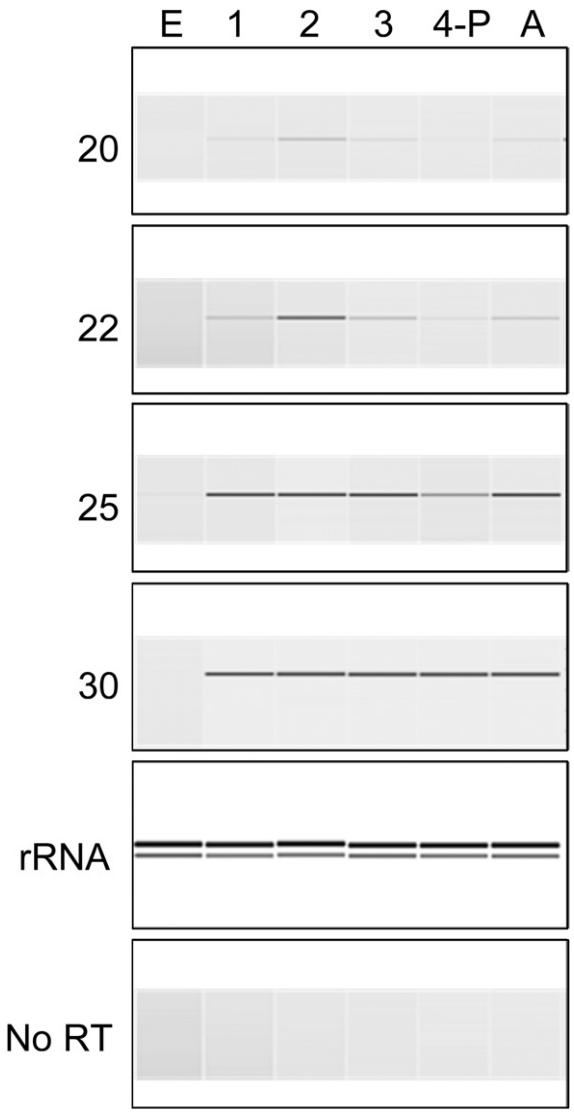

Fig. 3. Expression of *BtAQP1* in *B. tabaci* developmental stages. cDNA was prepared from 1.5 μg of total RNA from eggs (E), 1st instar crawlers (1), 2nd instar nymphs (2), 3rd instar nymphs (3), 4th instar nymphs and pupae (4-P), and adults (A). Two microliters of each RT reaction was PCR amplified and 1.0 μL of BtAQP1 RT-PCR product was analyzed on Agilent 2100 Bioanalyzer. An electronic gel image of the BtAQP1 PCR product at cycles (20, 22, 25 and 30) is shown. Ribosomal RNA (rRNA) from each stage is shown as internal control. The final panel shows a mock RT reaction lacking reverse transcriptase (No RT).

least three subfamilies (DRIPs, BIBs, and PRIPs) identified from insects (Campbell et al., 2008). Five to seven distinct AQPs have been identified in those insects with completed genomes (Campbell et al., 2008). Insect DRIPs are water-specific AQPs and are generally associated with fluid homeostasis by moving water through tissues for excretory purposes and/or maintenance of osmotic potential. BIBs do not transport water, but rather function as monovalent cation channels in nervous tissue (Yanochko and Yool, 2002). Insect PRIPs are not well characterized but at least one (PvAQP1) is involved in rapid dehydration and rehydration of *Polypedilum vanderplanki* under times of extreme environmental water stress (Kikawada et al., 2008).

Insect DRIPs share significant sequence similarity (Supplemental Fig. S2), topology (Fig. 1B), and predicted tertiary structure (Fig. 1C) with vertebrate AQPs (Beuron et al., 1995; Campbell et al., 2008; Elvin et al., 1999; Kataoka et al., 2009; Kaufmann et al., 2005; LeCaherec et al., 1996; Pietrantonio et al., 2000; Shakesby et al., 2009; Thomas et al., 2002). The pore within vertebrate AQPs is restricted by four residues (Phe, His, Cys, and Arg) that comprise the Ar/R constriction site (Sui et al., 2001). The Ar/R constriction residues are conserved in the BtAQP1, with the exception of Ala-207 in Loop E. This site contains a cysteine in several human AQPs (AQP-1, 2, 5, 6, and 9), whereas alanine or serine is found in other AQPs (Ala in human AQP-0 and 4, DmDRIP, AeaDRIP, and HieDRIP; Ser in ApAQP1, AmDRIP, BmDRIP, TcDRIP, and AQPcic) (Supplemental Figs. S1 and S2). BtAQP1 also possess the two NPA motifs important for water-selective permeation through the pore (Horsefield et al., 2008; Hub and De Groot, 2008; Murata et al., 2000; Sui et al., 2001) and are important in targeting AQPs to the plasma membrane (Guan et al., 2010).

BtAQP1 cRNA-injected *Xenopus* oocytes were significantly more permeable to water than control oocytes, indicating that BtAQP1 is a functional water transport protein comparable to human AQP1 (Preston et al., 1992). Oocytes injected with BtAQP1 cRNA did not show any appreciable transport of glycerol, consistent with the presence of a conserved pattern of Ar/R residues His-198 and Arg-213 in BtAQP1 that is characteristic of water-selective aquaporins (Sui et al., 2001; Thomas et al., 2002). Glycerol permeability remains to be demonstrated for insect AQPs (Campbell et al., 2008; Spring et al., 2009). To date, all insect DRIPs [AQPcic (LeCaherec et al., 1997), AeaAQP (Duchesne et al., 2003), and ApAQP1 (Shakesby et al., 2009)] including BtAQP1 have shown inhibition of water permeability in *Xenopus* oocytes in the presence of mercurials. BtAQP1 is therefore a member of the insect DRIP subfamily, which consists of water-specific channel proteins that transport water across lipid membranes for osmoregulatory, excretory and/or respiratory purposes.

The mercury sensitivity in human AQP1 and AQP2 is attributed to binding to Cys-189 and Cys-181, respectively with both residues located in extracellular loop E and in close proximity to the pore (Bai et al., 1996; Mulders et al., 1997; Preston et al., 1993). None of the insect aquaporins identified so far possesses a cysteine at or near this position (compare Supplemental Figs. S1 and S2). Studies with other vertebrate AQPs indicate a correlation between a cysteine residue near the first NPA motif and mercury sensitivity (Jung et al., 1994; Kuang et al., 2001). Interestingly, Kuang et al. (2001) showed that the mercury insensitive AQP1 mutant C189S regained wild-type mercury sensitivity when Ala-73 located near the first NPA motif was substituted with cysteine. Alignments reveal a conserved cysteine is located two residues upstream of the first NPA motif in nearly all insect DRIPs including BtAQP1 (Cys-88 which corresponds to AQP1 Ala-73) (Supplemental Fig. S1) and may explain mercury sensitivity. Based on predicted topology and modeling, BtAQP1 Cys-88 is predicted to be near the cytoplasmic face of transmembrane helix TM2 (Fig. 1A) where it extends into the pore and could contact intracellular mercury.

Water permeability in some vertebrate AQPs is inhibited by TEA (Detmers et al., 2006; Yool et al., 2002). Tyr-186, 178 and 207 in human AQP1, 2, and 4, respectively are located in loop E and proposed to be important for this inhibitory activity (Brooks et al., 2000; Detmers et al., 2006) (Supplemental Fig. S2). However, the presence of a conserved Tyr in loop E alone may not be sufficient for TEA sensitivity and additional residues in loop C (Asp-128), E (Asp-185) and A (Tyr-37, Asn-42 and Thr-44) are important for TEA sensitivity in human AQP1 (Detmers et al., 2006) (Supplemental Fig. S2). In BtAQP1, Tyr-204 is conserved in loop E; however, water permeability in *Xenopus* oocytes injected with BtAQP1 cRNA was not inhibited by TEA (Fig. 7A). TEA insensitivity in BtAQP1-injected oocytes could be due to the lack of conservation of those additional residues as proposed by (Detmers et al., 2006) (Supplemental Fig. S1).

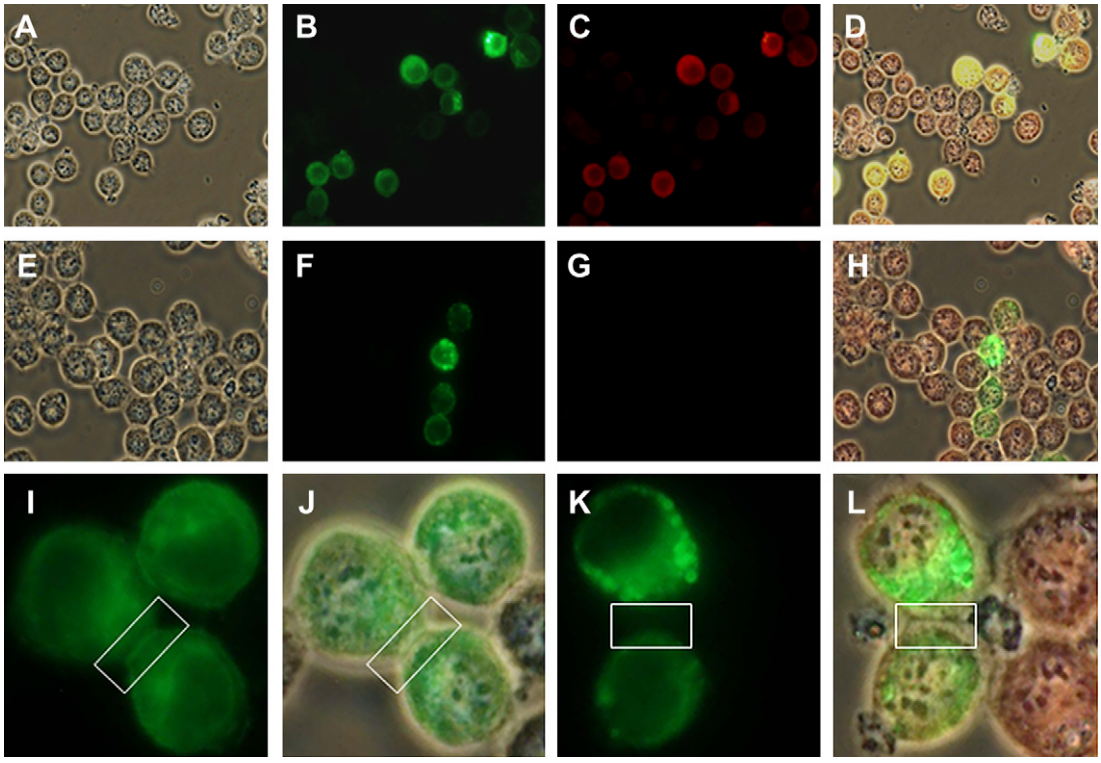

Fig. 4. Expression of recombinant BtAQP1 in Sf9 cells. (A–D) Sf9 cells transfected with eGFP-BtAQP1/pIB (full-length BtAQP1) were visualized under visible light (A), for direct GFP emission (B), or probed with anti-BtAQP1 antibody (C). (E–H) Sf9 cells transfected with eGFP-BtAQP1-TR#1/pIB (truncated BtAQP1 lacking 16 final carboxyl-terminal residues) were visualized under visible light (E), GFP (F), or probed with anti-BtAQP1 (G). GFP and BtAQP1 immunofluorescence were co-localized by direct overlay using the Olympus FSX 100 software (D and H). Cells transfected with full-length GFP-BtAQP1 show GFP-fluorescence on the entire cell surface (I and J), whereas fluorescence is primarily inside cells transfected with truncated GFP-BtAQP1 (K and L); compare boxes where plasma membranes of adjacent cells overlap, I and J (presence of fluorescence) with K and L (lack of fluorescence).

Levels of BtAQP1 transcripts differ during *B. tabaci* development indicating that protein expression likely changes throughout development (Fig. 3). The peak expression observed in the 2nd instar stage correlates with whitefly feeding behavior as BtAQP1 transcripts are most abundant after the nymphs have located a feeding site and are actively engaged in feeding on phloem. Because 1st instar nymphs must search for a feeding site, which can take up to 24 h (Borror et al., 1981; Simmons, 2002), it seems possible that expression of BtAQP1 only occurs after dietary fluid intake has been initiated. Nothing is known about potential promoters and/or the control of water channel AQP gene expression in arthropods. Furthermore, BtAQP1 transcripts are less abundant during the last nymphal instar and pupal stage (a time of discontinued feeding and tissue reorganization) followed by an increase after adult eclosion.

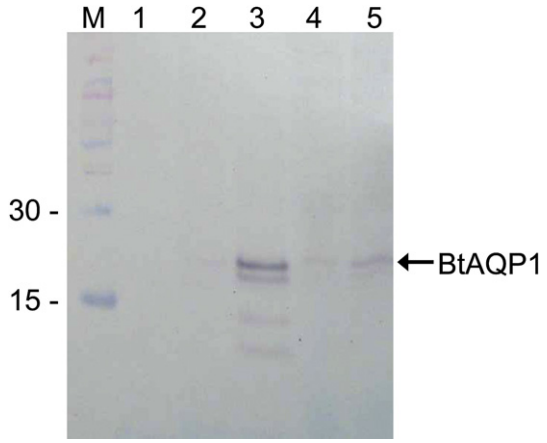

Fig. 5. Expression of BtAQP1 in *B. tabaci* tissues. Adults ($n = 40$) were dissected to obtain leg tissue (lane 1), heads (lane 2), intact gut tracts (lane 3), whole body minus gut (lane 4), and whole adult homogenates (lane 5). Each tissue homogenate (25 insect equivalents) were separated by SDS-PAGE and analyzed by immunoblotting with anti-BtAQP1. Lane M corresponds to Novex® Sharp Pre-Stained Protein Standard marker (Invitrogen). Arrow indicates putative full-length BtAQP1 from *B. tabaci* gut.

Because AQPs are integral transmembrane proteins that primarily function to transport water across cellular membranes, synthesis and transport to plasma membrane must occur. We show that intact recombinant BtAQP1 is localized to the plasma membrane of Sf9 cells and *Trichoplusia ni (T. ni)* cultured cells (data not shown). Similar observations have been reported in other aquaporins such as AQP4 (Yang et al., 1997). In producing a truncated BtAQP1 lacking the final 16 carboxyl-terminal residues to verify specificity of our antibody, we made an interesting observation that this region may be important for correct processing and targeting to the plasma membrane. Several potential phosphorylation sites are found in BtAQP1 (data not shown) that could be important for regulation of activity and/or membrane targeting. Most human AQPs are predominately expressed constitutively in cell-surface membranes, although differences exist in protein folding patterns and regulation of trafficking to membrane (Verkman and Mitra, 2000). The carboxyl-terminus of AQP4 has been previously shown to contain important signals for membrane targeting (Nakahama et al., 2002). Experiments are currently in progress to examine phosphorylation and to characterize our observation that the carboxyl-terminus of BtAQP1 is also important for membrane localization.

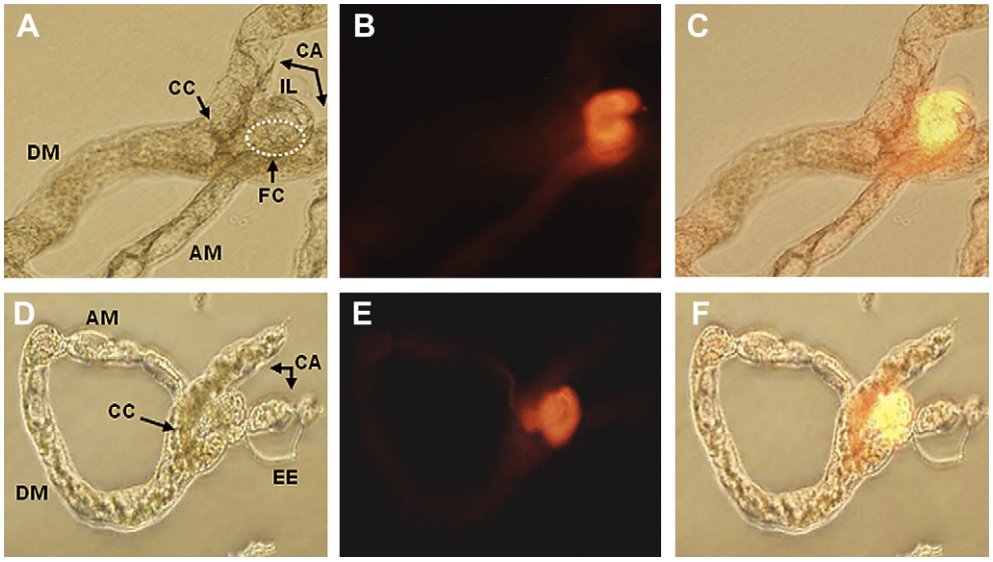

Fig. 6. Immunolocalization of BtAQP1 in *B. tabaci* gut. Fixed and permeabilized guts from *B. tabaci* adults ($n = 20$) were probed with anti-BtAQP1 and examined by immunofluorescence. Images of dissected alimentary tracts are shown as viewed from the dorsal (A–C) and ventral (D–F) side. (A) and (D) Visible image of adult *B. tabaci* gut showing external esophagus (EE), descending midgut (DM), ascending midgut (AM), connecting chamber (CC), filter chamber (FC), ileum (IL) of the hindgut and the caeca (CA). Note that FC and IL are not clearly visible from the ventral side and therefore not labeled in (D). (B) and (E) Immunofluorescence image (same as in A and D, respectively) showing BtAQP1 in filter chamber and ileum of the hindgut. (C) and (F) Overlay of visible and immunofluorescence images demonstrating expression of BtAQP1 in filter chamber and ileum of the hindgut with little or none in the EE, DM, AM, CC, or CA.

In adult *B. tabaci*, BtAQP1 is found primarily within the insect gut and more specifically in the filter chamber and the anterior ileum of the hindgut (Figs. 5 and 6). Anti-BtAQP1 antibody is highly specific to recombinant BtAQP1 expressed in cultured insect cells, and is immunogenic to protein found in the adult guts. Even though we expected BtAQP1 as a major protein band at 27 kDa, the anti-BtAQP1 cross reacted with a 22 kDa band and several smaller fragments. We speculate that one or more potential reasons contribute to this observation including non-serine-like proteolytic degradation despite addition of PMSF protease inhibitor, alternate transcriptional start site (at base 37 corresponding to Met-13), and/or anomalous SDS-PAGE migration due to variable detergent binding with helix-loop-helix structures (Rath et al., 2009).

Localization of BtAQP1 within the filter chamber and hindgut supports its potential role in transporting water across adjacent cell membranes within the filter chamber. A proposed function for the filter chamber involves rapidly arbitrating excess phloem sap water from the continuous lumen through the ascending midgut membrane via Malphigian-like tissue along an osmotic gradient between the filter chamber (a water shunting complex) and ileum of the hindgut, where water is ultimately excreted with honeydew or reabsorbed through the rectal sac (Ghanim et al., 2001). In the phloem-feeding cicadelloid leafhopper *Eurymela distincta* movement of water from lumen of filter chamber to the hindgut is thought to occur through passive osmosis enabled by secretion of Na^+ and K^+ ions into the lumen of the ascending midgut posterior to filter chamber and further reabsorption of these ions through the posterior ileum or rectal sac thereby forming an osmotic gradient (Lindsay and Marshall, 1981). The reduced osmotic pressure in liquid egesta and along the ileum and rectum (where ions are reabsorbed) indicates that this osmotic gradient is sufficient for water movement in the direction that favors excretion (Lindsay and Marshall, 1981). Other xylem and phloem-feeding insects use anatomically similar filter chamber structures to eliminate excess dietary fluids, including the phloem-feeding psyllids, which are thought to excrete excess sap components through a filter chamber directly into the hindgut (Cicero et al., 2009) and *C. viridis*, which uses AQPcic within the filter chamber for passive movement of water rapidly through the filter chamber into the hindgut (LeCaherec et al., 1996, 1997). However, in another phloem feeder, the aphid *A. pisum* which lacks a true filter chamber, the proposed direction of water movement is different. Based on the predicted osmotic potential within the *A. pisum* anterior midgut and hindgut, the net movement of water has been proposed to flow from the distal intestine to the stomach, resulting in dilution of fluid entering the midgut to protect the insect from osmotic dehydration (i.e. water cycling) (Ashford et al., 2000; Rhodes et al., 1997). Shakesby et al. (2009) proposes that in *A. pisum*, an AQP is involved in this rapid water movement based on tissue localization of ApAQP1 and due to the proposed osmotic gradient created by reduced osmotic pressure in the distal intestine resulting from sucrase-transglucosidase activity. A slight increase in hemolymph osmotic pressure in aphids presumably undergoing gene silencing of ApAQP1 was observed (Shakesby et al., 2009), suggesting that AQP function is important for osmotic regulation. To our knowledge, water cycling with a net flow of water from the ascending midgut through the filter chamber into the descending midgut has not been described in whiteflies, or in any other hemipteran phloem feeder other than *A. pisum*.

Phloem-feeding insects unlike xylem feeders are subjected to osmotic stress imposed by the high sucrose diet. Therefore, sugar transformation [a mechanism that involves the enzymatic conversion of sugar solutes from higher to lower osmotic pressure in order to reduce the osmolarity of phloem ingesta in insect phloem feeders (Douglas, 2006)] is considered to be crucial for osmoregulation. The enzymatic conversion of dietary disaccharides to oligosaccharides through monosaccharide intermediates reduces the osmotic pressure of the gut contents and prevents osmotic collapse in aphids (Rhodes et al., 1997; Ashford et al., 2000; Douglas, 2003). Similarly in whiteflies, the primary means of reducing osmotic pressure imposed by ingestion sucrose-rich phloem is thought to involve enzymatic conversion of sugars to ones that can be used for metabolism and/or thermotolerance, are readily excreted, or have reduced osmotic potential (Byrne et al.,

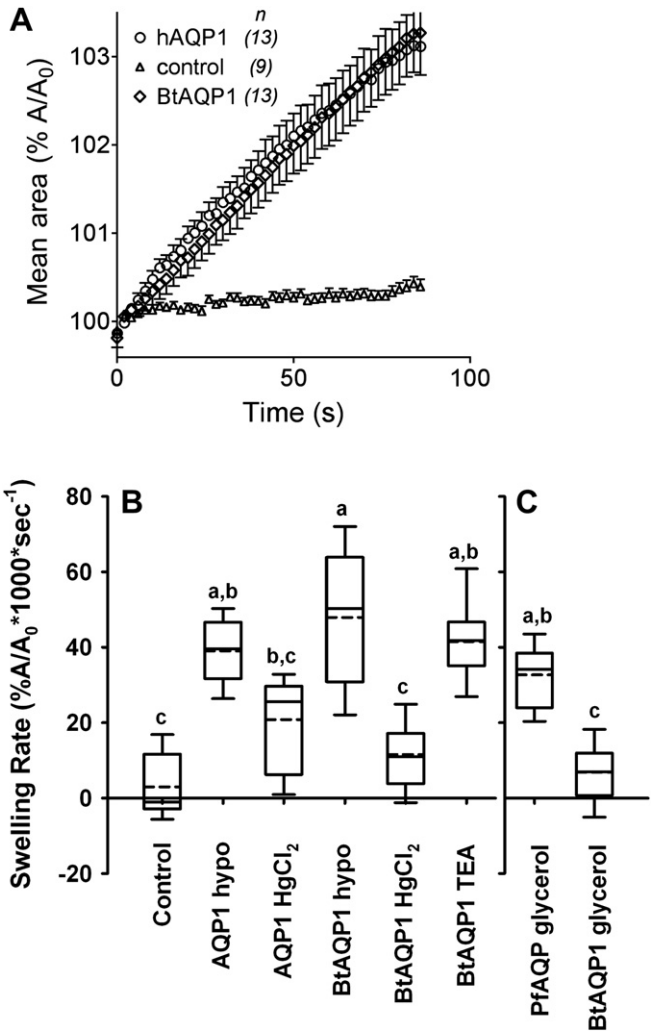

Fig. 7. Osmotic water and glycerol permeabilities of *Xenopus* oocytes expressing BtAQP1. (A) Representative examples of mean swelling rates (±SEM) of control, and AQP1- and BtAQP1-expressing oocytes as a function of time after introduction of oocytes into 50% hypotonic saline at time zero. Areas of the oocytes at each time point (A) are standardized to the initial area at time zero (Ao). (B) Complied data of swelling rates (slope values of linear regression fits of A/Ao versus time) reflecting water permeability of uninjected (Control), and human AQP1 (AQP1 hypo) and BtAQP1-expressing oocytes (BtAQP1 hypo) in untreated conditions treated with either 1 mM mercuric chloride ($HgCl_2$) or 100 μM tetraethylammonium (TEA). Defolliculated oocytes were injected with water (control) or 1 ng of cRNA and maintained in isotonic saline for 48 h prior to permeability measurements. Oocyte swelling was measured from volume changes recorded by video camera after transfer of oocytes to 50% hypotonic saline. (C) Compiled data of swelling rates reflecting glycerol permeability of BtAQP1 (BtAQP1 glycerol) and *Plasmodium falciparum* aquaglyceroporin (PfAQP glycerol). Glycerol permeability was measured in modified saline where glycerol iso-osmotically replaced 65 mM NaCl. Box plots show 25th and 75th quartiles (box), median (solid horizontal line within box), and mean (dotted horizontal line within box). Error bars represent SEM (n = 9–30). Data with the same letter were not significantly different (α = 0.05) as determined by the Kruskal–Wallis ANOVA on Ranks test.

2003; Hendrix and Brushwood, 2007; Hendrix and Salvucci, 2001, 1998; Salvucci, 2003; Salvucci and Crafts-Brandner, 2000; Salvucci et al., 1999, 1997; Wolfe et al., 1998). Thus, the role of sugar transformation and net osmotic potential of gut contents in adjacent intestinal tissues of phloem feeders is critical for understanding the net directional flow of water and hence the significance of water cycling or other methods of osmoregulation.

While the direction of water flow remains uncertain, current data suggest that AQPs are important for the mass transfer of water through adjoining gut tissue in phloem feeders. It is important to note that there are significant dietary, physiological, morphological, and biochemical differences between phloem feeders, any of which could contribute to overcoming osmotic challenges. Further study is needed to ascertain the net direction of water movement in phloem/xylem feeding arthropods and the physiological significance of such flow (osmotic regulation vs. nutrient concentration/excretion). The results presented here demonstrate that a water-specific aquaporin (BtAQP1) is present in the midgut filter chamber of *B. tabaci*, where it likely functions to transport water across Malphigian-like tissue located between ascending midgut and ileum of the hindgut tissues in order to provide osmotic stress relief or to remove excess dietary water for concentration of nutrients and efficient water excretion.

Acknowledgements

We thank J. Joe Hull for providing the pIB/EGFP plasmid and assistance with insect cell expression, Marcé Lorenzen for p3X3P3-eGFP plasmid, Peter Agre for human AQP1 cDNA, Eric Beitz for PfAQP cDNA, and Barbara Hefner for laboratory assistance and insect rearing. This is a cooperative investigation between USDA-ARS and the University of Adelaide. Mention of trade names or commercial products in this article is solely for the purpose of providing specific information and does not imply recommendation or endorsement by the U.S. Department of Agriculture.

Appendix. Supplemental data

Supplemental data related to this article can be found online at doi:10.1016/j.ibmb.2010.12.002.

References

Altschul, S.F., Gish, W., Miller, W., Myers, E.W., Lipman, D.J., 1990. Basic local alignment search tool. J. Mol. Biol. 215, 403–410.
Anthony, T.L., Brooks, H.L., Boassa, D., Leonov, S., Yanochko, G.M., Regan, J.W., Yool, A.J., 2000. Cloned human aquaporin-1 is a cyclic GMP-gated ion channel. Mol. Pharmacol. 57, 576–588.
Arnold, K., Bordoli, L., Kopp, J., Schwede, T., 2006. The SWISS-MODEL workspace: a web-based environment for protein structure homology modelling. Bioinformatics 22, 195–201.
Ashford, D.A., Smith, W.A., Douglas, A.E., 2000. Living on a high sugar diet: the fate of sucrose ingested by a phloem-feeding insect, the pea aphid *Acyrthosiphon pisum*. J. Insect Physiol. 46, 335–341.
Bai, L.Q., Fushimi, K., Sasaki, S., Marumo, F., 1996. Structure of aquaporin-2 vasopressin water channel. J. Biol. Chem. 271, 5171–5176.
Ball, A., Campbell, E.M., Jacob, J., Hoppler, S., Bowman, A.S., 2009. Identification, functional characterization and expression patterns of a water-specific aquaporin in the brown dog tick, *Rhipicephalus sanguineus*. Insect Biochem. Mol. Biol. 39, 105–112.
Benga, G., 2009. Water channel proteins (later called aquaporins) and relatives: past, present, and future. IUBMB Life 61, 112–133.
Beuron, F., Le Caherec, F., Guillam, M.T., Cavalier, A., Garret, A., Tassan, J.P., Delamarche, C., Schultz, P., Mallouh, V., Rolland, J.P., Hubert, J.F., Gouranton, J., Thomas, D., 1995. Structural analysis of a MIP family protein from the digestive tract of *Cicadella viridis*. J. Biol. Chem. 270, 17414–17422.
Boassa, D., Yool, A.J., 2003. Single amino acids in the carboxyl terminal domain of aquaporin-1 contribute to cGMP-dependent ion channel activation. BMC Physiol. 3, 12.
Borror, D.J., Delong, D.M., Triplehorn, C.A., 1981. An Introduction to the Study of Insects, sixth ed. Saunders College Publishing, Philadelphia.
Brooks, H.L., Regan, J.W., Yool, A.J., 2000. Inhibition of aquaporin-1 water permeability by tetraethylammonium: involvement of the loop E pore region. Mol. Pharmacol. 57, 1021–1026.
Byrne, D.N., Hendrix, D.L., Williams, L.H., 2003. Presence of trehalulose and other oligosaccharides in hemipteran honeydew, particularly Aleyrodidae. Physiol. Entomol. 28, 144–149.
Campbell, E.M., Ball, A., Hoppler, S., Bowman, A.S., 2008. Invertebrate aquaporins: a review. J. Comp. Physiol. B 178, 935–955.
Campbell, E.M., Burdin, M., Hoppler, S., Bowman, A.S., 2010. Role of an aquaporin in the sheep tick *Ixodes ricinus*: assessment as a potential control target. Int. J. Parasitol. 40, 15–23.

Cheung, W.W.K., Marshall, A.T., 1973. Water and ion regulation in *Cicadas* in relation to xylem feeding. J. Insect Physiol. 19, 1801–1816.
Cicero, J.M., Brown, J.K., Roberts, P.D., Stansly, P.A., 2009. The digestive system of *Diaphorina citri* and *Bactericera cockerelli* (Hemiptera: Psyllidae). Ann. Entomol. Soc. Am. 102, 650–665.
Cicero, J.M., Hiebert, E., Webb, S.E., 1995. The alimentary canal of *Bemisia tabaci* and *Trialeurodes abutilonea* (Homoptera, Sternorrhynchi) – histology, ultrastructure and correlations to function. Zoomorphology 115, 31–39.
Combet, C., Blanchet, C., Geourjon, C., Deleage, G., 2000. NPS@: network protein sequence analysis. Trends Biochem. Sci. 25, 147–150.
Combet, C., Jambon, M., Deleage, G., Geourjon, C., 2002. Geno3D: automatic comparative molecular modelling of protein. Bioinformatics 18, 213–214.
Detmers, F.J., de Groot, B.L., Muller, E.M., Hinton, A., Konings, I.B., Sze, M., Flitsch, S.L., Grubmuller, H., Deen, P.M., 2006. Quaternary ammonium compounds as water channel blockers. Specificity, potency, and site of action. J. Biol. Chem. 281, 14207–14214.
Douglas, A.E., 2003. The nutritional physiology of Aphids. Adv. Insect Physiol. 31, 73–140.
Douglas, A.E., 2006. Phloem-sap feeding by animals: problems and solutions. J. Exp. Bot. 57, 747–754.
Duchesne, L., Hubert, J.F., Verbavatz, J.M., Thomas, D., Pietrantonio, P.V., 2003. Mosquito (*Aedes aegypti*) aquaporin, present in tracheolar cells, transports water, not glycerol, and forms orthogonal arrays in Xenopus oocyte membranes. Eur. J. Biochem. 270, 422–429.
Echevarria, M., Ramirez-Lorca, R., Hernandez, C.S., Gutierriez, A., Mendez-Ferrer, S., Gonzalez, E., Toledo-Aral, J.J., Ilundain, A.A., Whittembury, G., 2001. Identification of a new water channel (Rg-MIP) in the Malpighian tubules of the insect *Rhodnius prolixus*. Pflug. Arch. Eur. J. Phy. 442, 27–34.
Elvin, C.M., Bunch, R., Liyou, N.E., Pearson, R.D., Gough, J., Drinkwater, R.D., 1999. Molecular cloning and expression in *Escherichia coli* of an aquaporin-like gene from adult buffalo fly (*Haematobia irritans exigua*). Insect Mol. Biol. 8, 369–380.
Fonseca, F.V., Silva, J.R., Samuels, R.I., DaMatta, R.A., Terra, W.R., Silva, C.P., 2010. Purification and partial characterization of a midgut membrane-bound alpha-glucosidase from *Quesada gigas* (Hemiptera: Cicadidae). Comp. Biochem. Phys. B 155, 20–25.
Ghanim, M., Rosell, R.C., Campbell, L.R., Czosnek, H., Brown, J.K., Ullman, D.E., 2001. Digestive, salivary, and reproductive organs of *Bemisia tabaci* (Gennadius) (Hemiptera: Aleyrodidae) B type. J. Morphol. 248, 22–40.
Gomes, D., Agasse, A., Thiébaud, P., Delrot, S., Gerós, H., Chaumont, F., 2009. Aquaporins are multifunctional water and solute transporters highly divergent in living organisms. Biochim. Biophys. Acta (BBA) .–Biomembranes 1788, 1213–1228.
Guan, X.G., Su, W.H., Yi, F., Zhang, D., Hao, F., Zhang, H.G., Liu, Y.J., Feng, X.C., Ma, T.H., 2010. NPA motifs play a key role in plasma membrane targeting of aquaporin-4. IUBMB Life 62, 222–226.
Gullan, P.J., Cranston, P.S., 2005. The Insects: An Outline of Entomology, third ed. Blackwell Publishing Ltd, Massachusetts.
Hansen, M., Kun, J.F., Schultz, J.E., Beitz, E., 2002. A single, bi-functional aquaglyceroporin in blood-stage *Plasmodium falciparum* malaria parasites. J. Biol. Chem. 277, 4874–4882.
Harris, K.F., Pesic Van Esbroeck, Z., Duffus, J.E., 1996. Morphology of the sweet potato whitefly, *Bemisia tabaci* (Homoptera, Aleyrodidae) relative to virus transmission. Zoomorphology 116, 143–156.
Hendrix, D.L., Salvucci, M.E., 1998. Polyol metabolism in homopterans at high temperatures: accumulation of mannitol in aphids (Aphididae: Homoptera) and sorbitol in whiteflies (Aleyrodidae: Homoptera). Comp. Biochem. Phys.–A 120, 487–494.
Hendrix, D.L., Salvucci, M.E., 2001. Isobemisiose: an unusual trisaccharide abundant in the silverleaf whitefly, *Bemisia argentifolii*. J. Insect Physiol. 47, 423–432.
Hendrix, D.L., Brushwood, D.E., 2007. Sweetpotato whitefly, bandedwinged whitefly and cotton aphid honeydew carbohydrates. In: Hequet, E., Henneberry, T.J., Nichols, R.L. (Eds.), Sticky Cotton – Causes, Impacts and Prevention. Agricultural Research Service Technical Bulletin No. 1915., United States Department of Agriculture, pp. 38–50.
Heymann, J.B., Engel, A., 1999. Aquaporins: phylogeny, structure, and physiology of water channels. News Physiol. Sci. 14, 187–193.
Hiroaki, Y., Tani, K., Kamegawa, A., Gyobu, N., Nishikawa, K., Suzuki, H., Walz, T., Sasaki, S., Mitsuoka, K., Kimura, K., Mizoguchi, A., Fujiyoshi, Y., 2006. Implications of the aquaporin-4 structure on array formation and cell adhesion. J. Mol. Biol. 355, 628–639.
Horsefield, R., Norden, K., Fellert, M., Backmark, A., Tornroth-Horsefield, S., van Scheltinga, A.C.T., Kvassman, J., Kjellbom, P., Johanson, U., Neutze, R., 2008. High-resolution x-ray structure of human aquaporin 5. Proc. Natl. Acad. Sci. USA 105, 13327–13332.
Hub, J.S., De Groot, B.L., 2008. Mechanism of selectivity in aquaporins and aquaglyceroporins. Proc. Natl. Acad. Sci. USA 105, 1198–1203.
Hubert, J.F., Thomas, D., Cavalier, A., Gouranton, J., 1989. Structural and biochemical observations on specialized membranes of the filter chamber, a water-shunting complex in sap-sucking homopteran insects. Biol. Cell 66, 155–163.
Ishibashi, K., Hara, S., Kondo, S., 2009. Aquaporin water channels in mammals. Clin. Exp. Nephrol. 13, 107–117.
Jung, J.S., Preston, G.M., Smith, B.L., Guggino, W.B., Agre, P., 1994. Molecular structure of the water channel through aquaporin CHIP. The hourglass model. J. Biol. Chem. 269, 14648–14654.
Kataoka, N., Miyake, S., Azuma, M., 2009. Aquaporin and aquaglyceroporin in silkworms, differently expressed in the hindgut and midgut of *Bombyx mori*. Insect Mol. Biol. 18, 303–314.
Kaufmann, N., Mathai, J.C., Hill, W.G., Dow, J.A.T., Zeidel, M.L., Brodsky, J.L., 2005. Developmental expression and biophysical characterization of a *Drosophila melanogaster* aquaporin. Am. J. Physiol.-Cell Physiol. 289, C397–C407.
Kiefer, F., Arnold, K., Kunzli, M., Bordoli, L., Schwede, T., 2009. The SWISS-MODEL repository and associated resources. Nucleic Acids Res. 37, D387–D392.
Kikawada, T., Saito, A., Kanamori, Y., Fujita, M., Snigorska, K., Watanabe, M., Okuda, T., 2008. Dehydration-inducible changes in expression of two aquaporins in the sleeping chironomid, *Polypedilum vanderplanki*. Biochim. Biophys. Acta (BBA)–Biomembranes 1778, 514–520.
Kuang, K., Haller, J.F., Shi, G., Kang, F., Cheung, M., Iserovich, P., Fischbarg, J., 2001. Mercurial sensitivity of aquaporin 1 endofacial loop B residues. Protein Sci. 10, 1627–1634.
Larkin, M.A., Blackshields, G., Brown, N.P., Chenna, R., McGettigan, P.A., McWilliam, H., Valentin, F., Wallace, I.M., Wilm, A., Lopez, R., Thompson, J.D., Gibson, T.J., Higgins, D.G., 2007. Clustal W and clustal X version 2.0. Bioinformatics 23, 2947–2948.
Laskowski, R.A., Macarthur, M.W., Moss, D.S., Thornton, J.M., 1993. Procheck – a program to check the stereochemical quality of protein structures. J. Appl. Crystallogr. 26, 283–291.
LeCaherec, F., Deschamps, S., Delamarche, C., Pellerin, I., Bonnec, G., Guillam, M.T., Thomas, D., Gouranton, J., Hubert, J.F., 1996. Molecular cloning and characterization of an insect aquaporin – functional comparison with aquaporin 1. Eur. J. Biochem. 241, 707–715.
LeCaherec, F., Guillam, M.T., Beuron, F., Cavalier, A., Thomas, D., Gouranton, J., Hubert, J.F., 1997. Aquaporin-related proteins in the filter chamber of homopteran insects. Cell Tiss. Res. 290, 143–151.
Lehane, M.J., Billingsley, P.F., 1996. Biology of the Insect Midgut, first ed. Chapman and Hall, London.
Lindsay, K.L., Marshall, A.T., 1981. The osmoregulatory role of the filter-chamber in relation to phloem-feeding in *Eurymela distincta* (Cicadelloidea, Homoptera). Physiol. Entomol. 6, 413–419.
Marshall, A.T., Cheung, W.W.K., 1974. Studies on water and ion-transport in homopteran insects – ultrastructure and cytochemistry of Cicadoid and cercopoid malpighian tubules and filter chamber. Tissue & Cell 6, 153–171.
Maurel, C., Verdoucq, L., Luu, D.T., Santoni, V., 2008. Plant aquaporins: membrane channels with multiple integrated functions. Annu. Rev. Plant Biol. 59, 595–624.
Mulders, S.M., Rijss, J.P.L., Hartog, A., Bindels, R.J.M., VanOs, C.H., Deen, P.M.T., 1997. Importance of the mercury-sensitive cysteine on function and routing of AQP1 and AQP2 in oocytes. Am. J. Physiol. Renal Physiol. 42, F451–F456.
Murata, K., Mitsuoka, K., Hirai, T., Walz, T., Agre, P., Heymann, J.B., Engel, A., Fujiyoshi, Y., 2000. Structural determinants of water permeation through aquaporin-1. Nature 407, 599–605.
Nakahama, K., Fujioka, A., Nagano, M., Satoh, S., Furukawa, K., Sasaki, H., Shigeyoshi, Y., 2002. A role of the C-terminus of aquaporin 4 in its membrane expression in cultured astrocytes. Genes Cells 7, 731–741.
Peitsch, M.C., 1995. Protein modeling by e-mail. Nat Biotechnol. 13, 658–660.
Pietrantonio, P.V., Jagge, C., Keeley, L.L., Ross, L.S., 2000. Cloning of an aquaporin-like cDNA and *in situ* hybridization in adults of the mosquito *Aedes aegypti* (Diptera: Culicidae). Insect Mol. Biol. 94, 407–418.
Preston, G.M., Carroll, T.P., Guggino, W.B., Agre, P., 1992. Appearance of water channels in *Xenopus* oocytes expressing red cell CHIP28 protein. Science 256, 385–387.
Preston, G.M., Jung, J.S., Guggino, W.B., Agre, P., 1993. The mercury-sensitive residue at cysteine 189 in the CHIP28 water channel. J. Biol. Chem. 268, 17–20.
Rath, A., Glibowicka, M., Nadeau, V.G., Chen, G., Deber, C.M., 2009. Detergent binding explains anomalous SDS-PAGE migration of membrane proteins. Proc. Natl. Acad. Sci. U S A 106, 1760–1765.
Rhodes, J.D., Croghan, P.C., Dixon, A.F.G., 1997. Dietary sucrose and oligosaccharide synthesis in relation to osmoregulation in the pea aphid, *Acyrthoslphon pisum*. Physiol. Entomol. 22, 373–379.
Rosell, R.C., Davidson, E.W., Jancovich, J.K., Hendrix, D.L., Brown, J.K., 2003. Size limitations in the filter chamber and digestive tract of nymphal and adult *Bemisia tabaci* whiteflies (Hemiptera: Aleyrodidae). Ann. Entomol. Soc. Am. 96, 544–552.
Roy, A., Kucukural, A., Zhang, Y., 2010. I-TASSER: a unified platform for automated protein structure and function prediction. Nat. Protoc 5, 725–738.
Saitou, N., Nei, M., 1986. Strategy for resolving the branching order of humans, chimpanzees and gorillas by using DNA-sequence data. Am. J. Phys. Anthropol. 69, 260.
Saitou, N., Nei, M., 1987. The neighbor-joining method - a new method for reconstructing phylogenetic trees. Mol. Biol. Evol. 4, 406–425.
Salvucci, M.E., 2003. Distinct sucrose isomerases catalyze trehalulose synthesis in whiteflies, *Bemisia argentifolii*, and *Erwinia rhapontici*. Comp. Biochem. Phys. B 135, 385–395.
Salvucci, M.E., Crafts-Brandner, S.J., 2000. Effects of temperature and dietary sucrose concentration on respiration in the silverleaf whitefly, *Bemisia argentifolii*. J. Insect Physiol. 46, 1461–1467.
Salvucci, M.E., Hendrix, D.L., Wolfe, G.R., 1999. Effect of high temperature on the metabolic processes affecting sorbitol synthesis in the silverleaf whitefly, *Bemisia argentifolii*. J. Insect Physiol. 45, 21–27.

Salvucci, M.E., Wolfe, G.R., Hendrix, D.L., 1997. Effect of sucrose concentration on carbohydrate metabolism in *Bemisia argentifolii*: biochemical mechanism and physiological role for trehalulose synthesis in the silverleaf whitefly. J. Insect Physiol. 43, 457–464.

Salvucci, M.E., Wolfe, G.R., Hendrix, D.L., 1998. Purification and properties of an unusual NADPH-dependent ketose reductase from the silverleaf whitefly. Insect Biochem. Mol. Biol. 28, 357–363.

Shakesby, A.J., Wallace, I.S., Isaacs, H.V., Pritchard, J., Roberts, D.M., Douglas, A.E., 2009. A water-specific aquaporin involved in aphid osmoregulation. Insect Biochem. Mol. Biol. 39, 1–10.

Simmons, A.M., 2002. Settling of crawlers of *Bemisia tabaci* (Homoptera: Alcyrodidae) on five vegetable hosts. Ann. Entomol. Soc. Am. 95, 464–468.

Sneath, Sokal, 1973. Numerical Taxonomy. W.H. Freeman and Company, San Francisco, pp. 230–234.

Spring, J.H., Robichaux, S.R., Hamlin, J.A., 2009. The role of aquaporins in excretion in insects. J. Exp. Biol. 212, 358–362.

Sui, H., Han, B.G., Lee, J.K., Walian, P., Jap, B.K., 2001. Structural basis of water-specific transport through the AQP1 water channel. Nature 414, 872–878.

Tamura, K., Dudley, J., Nei, M., Kumar, S., 2007. MEGA4: molecular evolutionary genetics analysis (MEGA) software version 4.0. Mol. Biol. Evol. 24, 1596–1599.

Thomas, D., Bron, P., Ranchy, G., Duchesne, L., Cavalier, A., Rolland, J.P., Raguenes-Nicol, C., Hubert, J.F., Haase, W., Delamarche, C., 2002. Aquaglyceroporins, one channel for two molecules. Biochim. Biophys. Acta 1555, 181–186.

Verkman, A.S., Mitra, A.K., 2000. Structure and function of aquaporin water channels. Am. J. Physiol. Renal Physiol. 278, F13–F28.

Wolfe, G.R., Hendrix, D.L., Salvucci, M.E., 1998. A thermoprotective role for sorbitol in the silverleaf whitefly, *Bemisia argentifolii*. J. Insect Physiol. 44, 597–603.

Yang, B., van Hoek, A.N., Verkman, A.S., 1997. Very high single channel water permeability of aquaporin-4 in baculovirus-infected insect cells and liposomes reconstituted with purified aquaporin-4. Biochemistry 36, 7625–7632.

Yanochko, G.M., Yool, A.J., 2002. Regulated cationic channel function in *Xenopus* oocytes expressing *Drosophila* big brain. J. Neurosci. 22, 2530–2540.

Yool, A.J., 2007. Functional domains of aquaporin-1: keys to physiology, and targets for drug discovery. Curr. Pharm. Des. 13, 3212–3221.

Yool, A.J., Brokl, O.H., Pannabecker, T.L., Dantzler, W.H., Stamer, W.D., 2002. Tetraethylammonium block of water flux in aquaporin-1 channels expressed in kidney thin limbs of Henle's loop and a kidney-derived cell line. BMC Physiol. 2, 4.

Zhang, Y., 2008. I-TASSER server for protein 3D structure prediction. BMC Bioinformatics 9, 40.

Zhang, Y., 2009. I-TASSER: fully automated protein structure prediction in CASP8. Proteins 77 (Suppl. 9), 100–113.